

# The Local Buckling of the Thin Walled Aluminium Mast

**Boris Jerman**

Assistant Professor  
University of Ljubljana  
Faculty of Mechanical Engineering

*In the paper a possible scenario for the occurrence of the local buckling of the wall of the thin walled aluminium mast is analysed. It is assumed that the hook of the auxiliary crane of the rubber-tired marine crane buckled to the lateral mast-supporting wire rope during the retrieval motion from the pier. The consequences of an unintended crane action on the mast of the sailing boat are studied using combination of analytical calculations and FEM. The complexity of the mast – mast wires system, the big displacements and non-linear material characteristics are taken into account. The properties of the tempered aluminium alloy are included as well as properties in the heat affected zone in the vicinity of the welds. On the basis of the calculated internal forces and moments in the mast and wire-ropes, the possibility of occurrence of different types of failure are studied. The estimated possible damages are compared with actual damages.*

**Keywords:** aluminium alloy, thin walled mast profile, local buckling.

## 1. INTRODUCTION

The transportation of the boats in the marines with rubber-tired marine cranes is a common routine procedure. When bigger sailing boats are in question a special precaution is needed regarding the mast(s) and mast-supporting steel wire-ropes.

In the paper an accident is studied involving an auxiliary boom crane mounted on the rubber-tired marine crane (Fig. 1a). After successful transportation of bigger sailing boat from the marine soil in to the water the marine crane started its retrieval motion from the pier. Because of the routine status of the procedure the crane's operator did not pay enough attention. The hook of the auxiliary crane (Fig. 1b) buckled to one of the left lateral mast-supporting wire-ropes between the lowest and the middle spar of the mast (Figs. 2 and 4). The crane prolonged its motion for a few more meters and overloaded the mast before it finally stands steel.

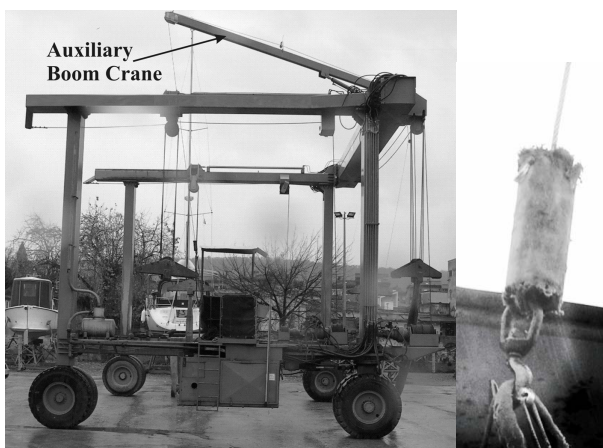


**Figure 1. The rubber-tired marine crane with auxiliary boom crane and its hook**

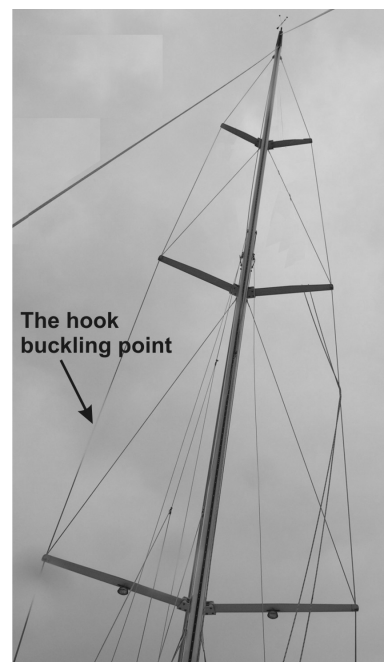


**Figure 2. The mast**

After the accident the partial extraction of the support of the lowest left spar from the mast profile was estimated immediately but, on the other hand, the local buckling of the mast profile's walls above the highest spar (Fig. 3) was not. After that, the question was raised if the buckling could be a consequence of the described accident or not.

In the literature the analytical and numeric approach to the analysis of the mast systems can be found. For the example Boote and Caponetto [1] used a numerical approach to the design of masts of the sailing boats. Jatulis et al. [2] performed a static behaviour analysis of masts with combined guys. The purpose of the study was to develop a new type of guyed mast that incorporates a complex guy cable system with a particular focus on the effect of static loading on the mast response behaviour. Enlund et al. [3] were researching the stresses in the mast and rigging of a

Received: February 2010, Accepted: March 2010

Correspondence to: Dr Boris Jerman  
Faculty of Mechanical Engineering,  
Aškerčeva 6, 1000 Ljubljana, Slovenia  
E-mail: boris.jerman@fs.uni-lj.si

sailing boat during sailing. The loading of the sails was defined using the pressure distributions based on know lift and drag coefficients of sails. During the research the analytical and numerical approaches were used as was the experiment. Atkinson [4] used finite element techniques, developed for analysing the marine propellers, for researching the boat's sails. Structural and aerodynamic calculations of sails as flexible members were done by Schop and Hansel [5] who also used numerical simulations.



Figure 3. The local buckling of the mast

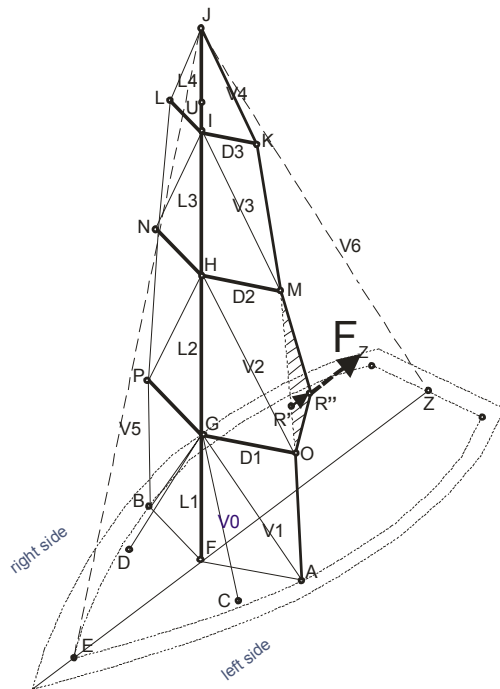


Figure 4. The sketch of the FEM model of the mast system

As can be seen from the stated literature the mast system is too complex for the pure analytical approach. On the other hand, in the current research also the experimental approach was not possible. Therefore, the described accident was theoretically examined by means of analytical approach combined with the numerical finite element method (FEM).

## 2. THE FEM MODEL

In the FEM model of the sailing-boat's mast system the complexity of the mast – mast wires system, the big

displacements and non-linear material characteristics of the tempered aluminium alloy are taken into account. The force  $F_z$  resulting from the unintended crane action is applied to the FEM model shown in Figure 5 and schematically presented in Figure 4. The finite elements of a "beam" and "spar" type are used.

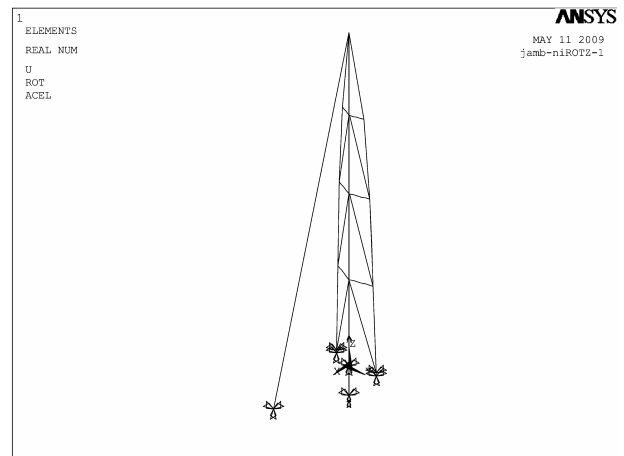


Figure 5. The FEM model of the mast system

### 2.1 The input data

The observed mast system is shown in Figure 2 and also presented in Figure 4. Three spars are dividing the mast into four sections of the lengths:  $L_1 = 5.8$  m,  $L_2 = 5.7$  m,  $L_3 = 5.4$  m and  $L_4 = 5.3$  m. The spars' lengths are defined by dimensions:  $D_1 = 1.6$  m,  $D_2 = 1.3$  m and  $D_3 = 0.9$  m. Other relevant distances are  $\overline{EF} = 5.9$  m,  $\overline{AB} = 3.2$  m,  $\overline{CD} = 2.7$  m and  $\overline{BC} = 3.2$  m.

In the FEM model, besides the mast with the spars, the wire-ropes from V1 to V5 are also considered, whereas the ropes V0 and V6 are not. The fixing points C and D of the ropes V0 are too deformable to allow for these ropes to have noticeable influence, and the rope V6 is not in place during the transportation of the sailing-boat by the marine crane. All the ropes are of the type 1 × 19 (1 + 6 + 12) according to [6], made from stainless steel with the ultimate strength of 1570 MPa. The ropes V1 to V3 are of the diameter 10 mm and the ropes V4 and V5 of the diameter 12 mm.

The mast is produced from the Bamar hollow profile BM94 [7] with the following properties:  $H = 270$  mm,  $B = 145$  mm, the thickness  $t = 5$  mm, the minimum thickness  $t_{\min} = 4.25$  mm (considering the possible tolerance of - 15 %), the cross section  $A = 3500$  mm<sup>2</sup>, the minimum cross section  $A_{\min} = 2975$  mm<sup>2</sup> (considering the possible tolerance of - 15 %), the moments of inertia  $I_y = 3114$  cm<sup>4</sup> and  $I_z = 1006$  cm<sup>4</sup>. The material of the mast is an aluminium alloy 6061 T6 with the following properties [8]: the yield strength is  $\sigma_y = 240$  MPa, the ultimate strength is  $\sigma_u = 260$  MPa and the Young's module is  $E = 69000$  MPa.

### 2.2 The loading

The FEM model of a mast system is firstly preloaded by means of the pre-stressed wire-ropes. The amount of the pre-stress in the individual wire-rope is defined as a 10 % of its ultimate strength.

After that the force  $F_z$  is applied onto the wire-rope V4 at the point R' where the hook of the auxiliary crane buckled during the accident.

Although the point of insertion and the direction of the action were known, the amplitude of the force was not. The amplitude of the  $F_z$  (Fig. 4) is therefore defined as a force which produces adequate loading  $F_O$  of the lowest left spar  $D_1$  in the outer point O of the spar (where the rope V4 is guided) to cause the partial extraction of the support of the spar from the mast profile, which was noticed after the accident.

For these reasons, firstly the FEM analysis was performed, where the magnitude of the force  $F_z$  was changing from zero to 40 kN. The results of this analysis are the values of the force  $F_O$ , which acts in the point O and produces the bending moment in the spar  $D_1$ . This force was then used in the following analytical expression:

$$\tau_{shr} = \frac{M_{up}}{W_{X,shr}} = \frac{F_O \cdot D_1}{W_{X,shr}} = \tau_{u,shr,haz}, \quad (1)$$

where  $\sigma_{u,haz} = 210$  MPa is a reduced ultimate strength of the aluminium alloy of the mast profile in the heat affected cone (HAZ) caused by the welding [10],  $W_{X,shr} = 169 \cdot 10^3$  mm<sup>3</sup> is a (shear) resistance moment of the mast profile wall in vicinity of the weld (see dashed line along the weld in Figure 6) and:

$$\tau_{u,shr,haz} = \frac{\sigma_{u,haz}}{\sqrt{3}} = 121 \text{ MPa} \quad (2)$$

is a reduced ultimate shear strength of the mast profile wall in HAZ.

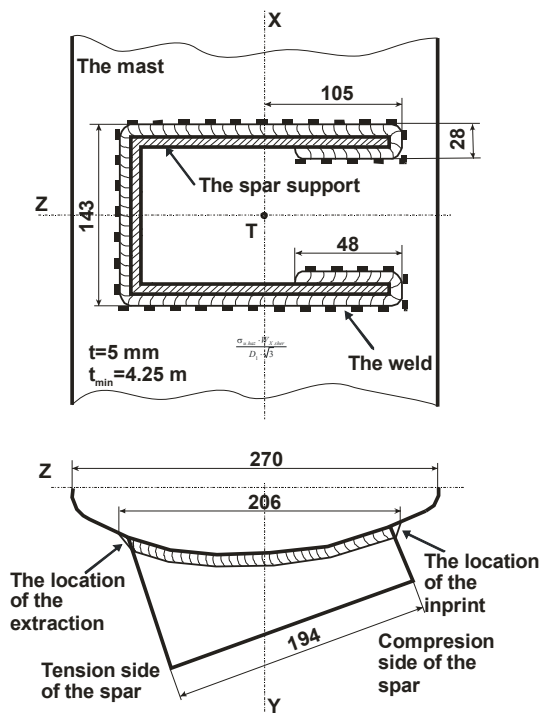


Figure 6. The spar support, welded onto the mast

From (1) the maximum shear stress in the described section of the mast profile can be calculated for any value of the force  $F_O$ . It is furthermore assumed that the shear stress must be equivalent to the ultimate shear

strength for extraction of the support to (almost) take place.

By considering the above information, the following diagram (Fig. 7) is calculated, from which the corresponding interval of the value of the force  $F_{z,extr}$  is determined as:

$$29 \text{ kN} \leq F_{z,extr} \leq 36.5 \text{ kN} . \quad (3)$$

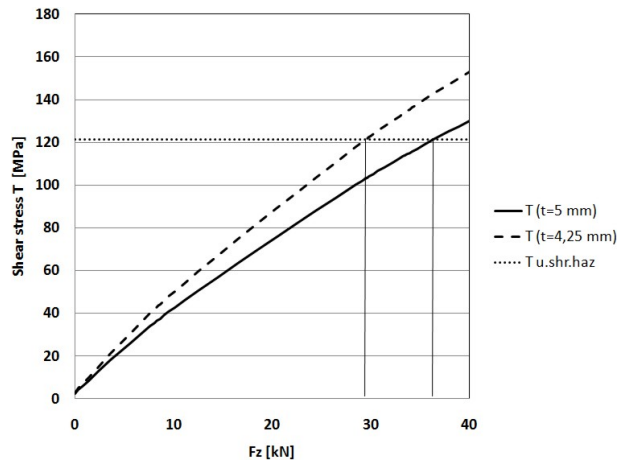


Figure 7. The diagram of shear stresses in the mast wall

The lower value is for the case of the thinnest wall possible ( $t = 4.25$  mm) and the highest is for the nominal wall thickness of the mast profile of  $t = 5$  mm. The interval defined in (3) is therefore the interval of the crane force in which the extraction of the spar support is to be expected.

### 2.3 Results of the FEM analysis

The sample results of internal moments  $M_y$  and  $M_z$  in the elements of the mast system are shown in the Figures 8 and 9 for the value of force  $F_{z,extr} = 29$  kN. From these diagrams the course of both the moments along the mast's length can be read out. For further research the information from a few characteristic points is used which will be shown in diagrams in the next section.

The FEM model is used furthermore to estimate the ranges of values of internal forces and moments in the mast, spars and wires, corresponding to the relevant interval of force  $F_z$ . These results are used in further calculations, as presented in the next paragraph.

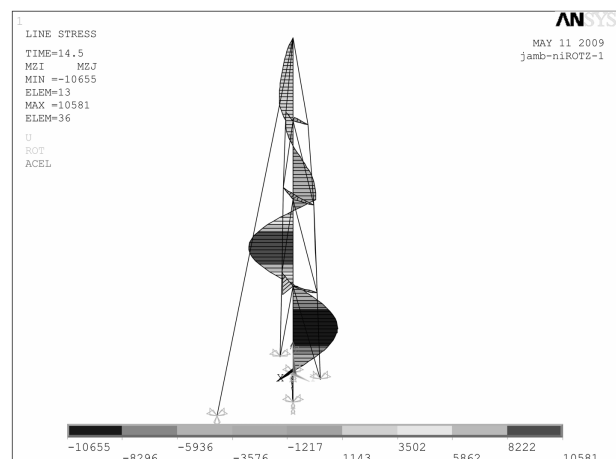


Figure 8. Bending moments  $M_z$  in the mast ( $F_{z,extr} = 29$  kN)

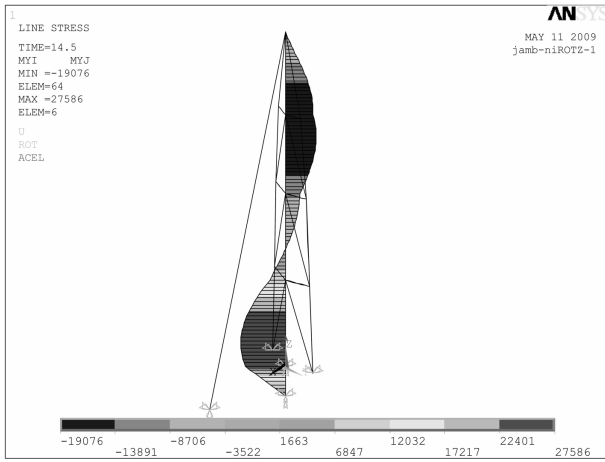


Figure 9. Bending moments  $M_z$  in the mast ( $F_{z,extr} = 29$  kN)

### 3. THE ANALYTICAL CALCULATIONS

With the intention to check the possibilities of plasticization of the mast profile, of global buckling of the profile, and of local buckling of the mast profile's walls the appropriate ultimate limit values are defined analytically for the members of interest.

The variations of the properties of the tempered aluminium alloy in the HAZ in the vicinity of the welds are included where necessary as well as the variations in thickness  $t$  of the profile walls. Where it is important the contraction of the top section of the mast (Fig. 10) is also taken into account as well as the residual stresses in the profile of that section in the vicinity of the longitudinal welds (Fig. 10).

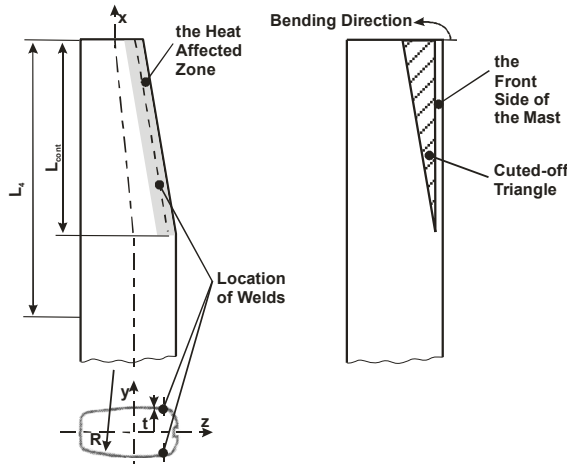


Figure 10. The mast cross-section and contraction of the top of the mast

The values of internal loads estimated by means of FEM analyses are then presented in the diagrams along the value of  $F_z$  together with the estimated ultimate limit values of these loads to enable the comparison of curves.

#### 3.1 The limit loading in the case of global buckling of the mast

The global buckling must be analysed considering the orientation of the profile cross-section and the effects of the lateral supports of the mast. The aim of this part of the investigation is to determine whether the global buckling occurs before or after the force  $F_z$  reaches the

limit value  $F_{z,extr}$ .

It is estimated that the global buckling around the weaker "z" axes (see Figure 10) of the mast cross-section is to be expected. Because of the effects of the lateral supports of the mast by means of the spars and wire-ropes and by means of the lower support the mast can be divided into four separate compression sections by the positions of three spars. It is assumed that the buckling length of separate sections is equal to the original lengths of these sections. The lowest section of the length  $L_1$  is the longest and also loaded with the biggest compression force and is therefore the most sensitive for the buckling.

The limit buckling force  $F_{g,bck.L1}$  for this element can be calculated:

$$i = \sqrt{\frac{I_z}{A}} = \sqrt{\frac{10060000}{3500}} = 53.61 \text{ mm}, \quad (4)$$

$$\lambda_1 = \frac{L_1}{i} = \frac{5800}{53.61} = 108.19, \quad (5)$$

$$\lambda_{pl} = \pi \cdot \sqrt{\frac{E}{\sigma_y}} = \pi \cdot \sqrt{\frac{69000}{240}} = 53.27, \quad (6)$$

$$\bar{\lambda}_1 = \frac{\lambda_1}{\lambda_{pl}} = \frac{108.19}{53.27} = 2.031, \quad (7)$$

$$\begin{aligned} \Phi &= 0.5 \cdot [1 + \alpha \cdot (\bar{\lambda}_1 - \lambda_0) + \bar{\lambda}_1^2] = \\ &= 0.5 \cdot [1 + 0.32 \cdot (2.031 - 0) + 2.031^2] = 2.887, \quad (8) \end{aligned}$$

$$\begin{aligned} K_1 &= \frac{1}{\Phi + \sqrt{\Phi^2 - \bar{\lambda}_1^2}} = \\ &= \frac{1}{2.887 + \sqrt{2.887^2 - 2.031^2}} = 0.2025, \quad (9) \end{aligned}$$

$$\begin{aligned} F_{g,bck.L1} &= K_1 \cdot A \cdot \sigma_y = \\ &= 0.2025 \cdot 3500 \cdot 240 = 170 \text{ kN}. \quad (10) \end{aligned}$$

Besides it also the highest mast section of the length  $L_4$  is observed. The limit buckling force  $F_{g,bck.L4}$  for this element can be calculated:

$$\lambda_4 = \frac{L_4}{i} = \frac{5300}{53.61} = 98.86, \quad (11)$$

$$\bar{\lambda}_4 = \frac{\lambda_4}{\lambda_{pl}} = \frac{98.86}{53.27} = 1.856, \quad (12)$$

$$\begin{aligned} \Phi_4 &= 0.5 \cdot [1 + \alpha \cdot (\bar{\lambda}_4 - \lambda_0) + \bar{\lambda}_4^2] = \\ &= 0.5 \cdot [1 + 0.32 \cdot (1.856 - 0) + 1.856^2] = 2.519, \quad (13) \end{aligned}$$

$$\begin{aligned} K_4 &= \frac{1}{\Phi_4 + \sqrt{\Phi_4^2 - \bar{\lambda}_4^2}} = \\ &= \frac{1}{2.519 + \sqrt{2.519^2 - 1.856^2}} = 0.237, \quad (14) \end{aligned}$$

$$F_{g.bck.L4} = K_4 \cdot A \cdot \sigma_y = 0.237 \cdot 3500 \cdot 240 = 199 \text{ kN} . \quad (15)$$

### 3.2 The limit loading in the case of local buckling of the profile walls

The limit local buckling load of the mast walls is calculated as the loading which must appear on the wall of the cylinder shell [9] of the radius  $R = 600$  mm, which is the radius of the mast profile (see  $R$  in Figure 10).

To finally calculate the limit stress by (16) for  $t = 5$  mm:

$$\sigma_{l.bck.Li} = (1 - 0.4123 \cdot \bar{\lambda}^{1.2}) \cdot \sigma_y = (1 - 0.4123 \cdot 1.110^{1.2}) \cdot 240 = 127.8 \text{ MPa} , \quad (16)$$

the following coefficients are defined first:

$$8 \cdot \sqrt{\frac{t}{R}} = 8 \cdot \sqrt{\frac{5}{600}} = 0.730 , \quad (17)$$

$$0.95 \cdot \sqrt{\frac{R}{t}} = 0.95 \cdot \sqrt{\frac{600}{5}} = 10.41 , \quad (18)$$

$$\sigma_{kr} = \frac{E}{\sqrt{3 \cdot (1 - \mu^2)}} \cdot \frac{t}{R} = \frac{69000}{\sqrt{3 \cdot (1 - 0.3^2)}} \cdot \frac{5}{600} = 348 \text{ MPa} . \quad (19)$$

$$\bar{\lambda} = \sqrt{\frac{\sigma_y}{\alpha_0 \cdot \sigma_{kr}}} = \sqrt{\frac{240}{0.560 \cdot 348}} = 1.110 < \sqrt{2} , \quad (20)$$

$$\alpha_0 = \frac{0.83}{\sqrt{1 + 0.01 \cdot \frac{R}{t}}} = \frac{0.83}{\sqrt{1 + 0.01 \cdot \frac{600}{5}}} = 0.560 . \quad (21)$$

Because the actual thickness of the walls is unknown the minimum possible thickness  $t_{\min} = 4.25$  mm must also be considered and the following modified limit stress is obtained:

$$\sigma_{l.bck.kor.Li} = (1 - 0.4123 \cdot \bar{\lambda}^{1.2}) \cdot \sigma_y = (1 - 0.4123 \cdot 1.232^{1.2}) \cdot 240 = 112.8 \text{ MPa} . \quad (22)$$

### 3.3 The limit compression loading

The yield strength of the mast's aluminium alloy  $\sigma_y = 240$  MPa represents the limit stress for the common compression loading in the section  $L_1$  of the mast. This value applies to the section  $L_4$  too because of the area where the yield strength is reduced by means of welding is too small to effect the load-bearing capacity. On the other hand the residual stresses due to longitudinal welds in this section must be considered.

### 3.4 The residual stresses caused by welding

During the welding of the longitudinal welds (Fig. 10) the residual stresses are inserted into the structure. In the fusion zone the tensile stresses remain causing the compression residual stresses in the vicinity of that zone.

The mentioned residual compression stresses are approximated by the following formulae:

$$\sigma_{cmp.res} = \frac{F_{ten.res}}{A_{cmp}} = \frac{2 \cdot b_{ten} \cdot t \cdot \sigma_{y.haz}}{A - 2 \cdot b_{ten} \cdot t} = \frac{2 \cdot 10 \cdot 5}{3500 - 2 \cdot 10 \cdot 5} \cdot 120 = 3.53 \text{ MPa} , \quad (23)$$

where the  $F_{ten.res}$  is a residual tension force in the fusion zone of the weld under the assumption that the maximal possible tension stress is inserted which equals to the reduced yield stress  $\sigma_{y.haz} = 120$  MPa [10]. The  $A_{cmp}$  is a cross-section of the profile reduced for a tensional loaded part in vicinity of the weld:

$$A_{cmp} = A - 2 \cdot b_{ten} \cdot t . \quad (24)$$

In (23) and (24) the  $b_{ten} \approx 2 \cdot t = 10$  mm is the assumed width of the tension zone in HAZ.

Because the longitudinal welds are located on the side of the profile (Fig. 11), besides the pure compression, the residual bending moment is also introduced.

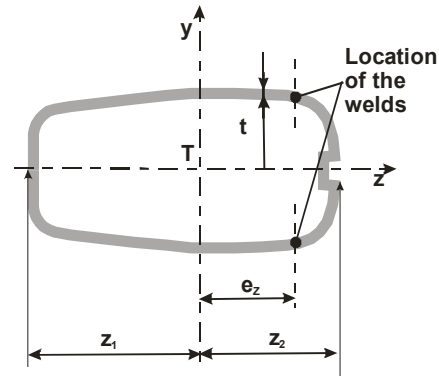


Figure 11. The location of welds in the mast cross-section

The residual bending stresses are calculated:

$$\sigma_{bnd.res} = \frac{F_{ten.res} \cdot e_z}{W_{y,2.mast}} = \frac{(\sigma_{y.haz} \cdot b_{ten} \cdot t \cdot 2) \cdot e_z}{W_{y,2.mast}} = \frac{120 \cdot 10 \cdot 5 \cdot 2 \cdot 97.7}{2.366 \cdot 10^5} = 5.00 \text{ MPa} , \quad (25)$$

where  $W_{y,2.mast}$  is the resistance moment of the cross-section of the profile reduced for a part in vicinity of the weld which is in tension. The  $e_z$  is a distance from the centre of gravity  $T$  to the position of the welds (Fig. 11).

Calculated residual stresses are combined together in two ways. The contribution of these stresses to the total compression stress is:

$$\sigma_{RES.CMP} = \sigma_{cmp.res} + \frac{3 \cdot \sigma_{bnd.res}}{4} = 3.53 + \frac{3 \cdot 5}{4} = 7.28 \text{ MPa} , \quad (26)$$

and contribution of these stresses to the local buckling stress is:

$$\begin{aligned}\sigma_{\text{RES.l.bck}} &= \sigma_{\text{cmp.res}} + \frac{\sigma_{\text{bnd.res}}}{2} = \\ &= 3.53 + \frac{5}{2} = 6.03 \text{ MPa}.\end{aligned}\quad (27)$$

#### 4. THE RESULTS

The results of the FEM analyses are the internal forces and moments in the mast system elements. These results are used for calculation of stresses in the mast profile. Further, the so obtained stresses are combined together for estimation of their common effects.

The distribution of these stresses along the mast cross-section is shown in a simplified manner in Figure 12, where the oval shape of the profile is presented as a rectangle. The simplification is adopted only for easier graphical presentation and does not effect the stress equations.

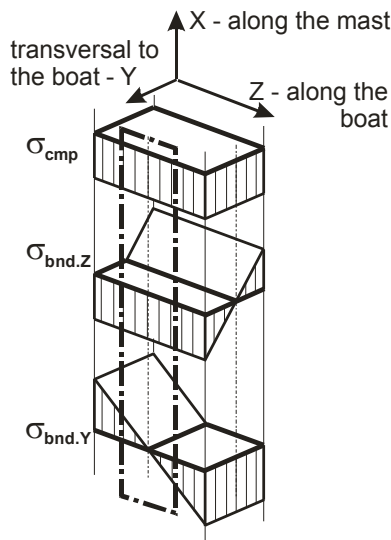


Figure 12. Approximate distribution of the stresses in the simplified mast cross-section

The total stress, which is significant for the occurrence of the common compression yielding, is assumed to be:

$$\sigma_{\text{cmp.total}} = \sigma_{\text{cmp}} + \sigma_{\text{bnd.z}} + \frac{3 \cdot \sigma_{\text{bnd.y}}}{4}, \quad (28)$$

where the oval shape of the profile is considered by means of the reduction factor  $\frac{3}{4}$ .

It is possible that during the overloading a partial plasticization of the mast cross-section occurred, which was not revealed because the elastically deformed parts of the cross-section managed to preserve the shape of the profile. In this case even higher stresses can be assumed, which is considered with additional reduction of stress components:

$$\sigma_{\text{cmp.total}*} = \sigma_{\text{cmp}} + \frac{\sigma_{\text{bnd.z}}}{1.1} + \frac{3 \cdot \sigma_{\text{bnd.y}}}{4 \cdot 1.35}. \quad (29)$$

In the Figure 12 the stresses which are significant for the occurrence of the local buckling are denoted with

centre line parallelogram. The total stress for the local buckling is then calculated as:

$$\sigma_{\text{l.bck.total}} = \sigma_{\text{cmp}} + \sigma_{\text{bnd.z}} + \frac{\sigma_{\text{bnd.y}}}{4}. \quad (30)$$

#### 4.1 The global buckling

In this section the possibility is examined if the actual compression forces exceed the limit buckling forces in the individual mast sections during the undesired event. The Figure 13 shows the diagram of the calculated internal axial compression forces in the sections  $L_1$  and  $L_4$  of the mast along the crane force  $F_z$ . The interval of  $F_{z,\text{extr}}$  is also shown in which the extraction of the spar carrier is expected to occur.

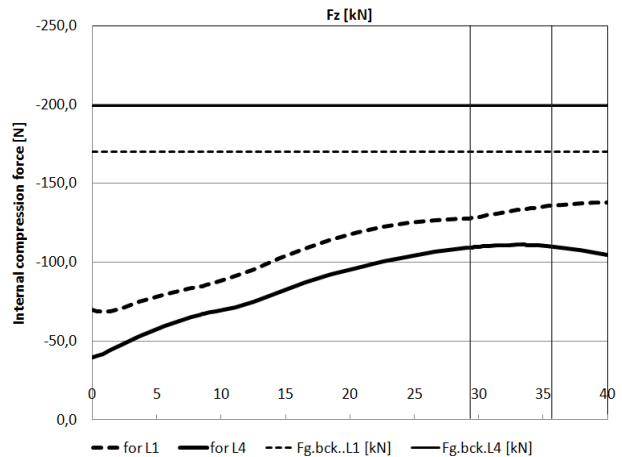


Figure 13. Axial compression forces in mast sections  $L_1$  and  $L_4$  and limit compression forces in these section

The graphs clearly show that none of the observed internal forces exceed or even reach the corresponding limit global buckling values in the observed case when the crane force  $F_z$  arise from zero to the extraction value  $F_{z,\text{extr}}$ .

This information confirms that the crane force needed for the extraction is too low to cause the global buckling. This leaves the gap for the possibility of occurrence of the detected local buckling.

#### 4.2 The local buckling

In this section the possibility is examined if the actual compression stresses in the walls of the mast profile exceed the limit local buckling stresses. The limit stress for the section  $L_4$  is decreased to consider the possibility that the thickness of walls there is minimal allowed  $t_{\text{min}}$ .

The actual stresses are shown for the location in the middle of the section  $L_1$ , for the point U (Fig. 4) where the contraction of the section  $L_4$  (Fig. 10) begins and for the location in the middle of the contracted part ( $l_{\text{cont}}$  in Figure 10) of the section  $L_4$ , where the cross-section of the mast profile is reduced.

When actual stresses are calculated in the section  $L_1$  the nominal thickness  $t$  is taken into account whereas in the case of  $L_4$  the reduced thickness  $t_{\text{min}}$  is used.

In section  $L_4$  where longitudinal welds are located also the effects of the residual compression stresses are taken into account.

The curves of the described stresses plotted along the crane force  $F_z$  are shown in Figure 14.

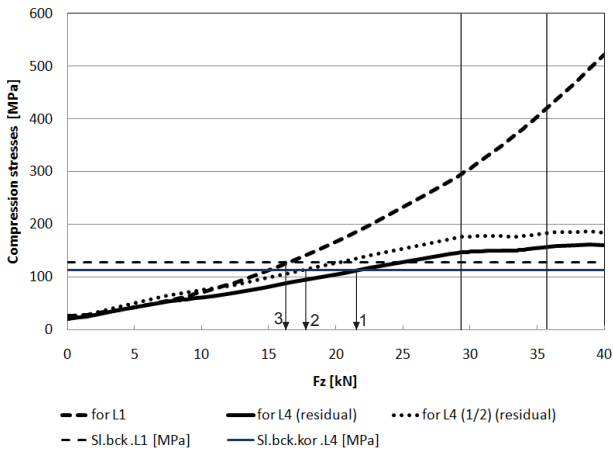


**Figure 14. Local buckling compression stresses in walls of the mast sections  $L_1$  and  $L_4$  and limit local buckling stresses in these section**

From the curves in Figure 14 the following conclusions are made. All the calculated actual stresses reach the corresponding limit local buckling values before the crane force reaches the extraction interval.

This conclusion still leaves the option of occurrence of the estimated local buckling open but on the other hand the further observations give us a different picture.

It is noticeable that the local buckling in section  $L_1$  would have occur at the lower stress (see arrow 3 in Figure 14) than in section  $L_4$  (see arrow 2 for the midpoint of the contracted part and arrow 1 for the point U, where the contraction of the profile begins).

The narrow position of the arrows 2 and 3 is leaving a slight possibility of occurrence of the assumed event under the assumption that these two values differs for less than is the precision of the presented calculation method.

### 4.3 The compression

In this section is examined if it is possible that the actual compression stress exceeds the yield stress of the involved material.

As before, also in this case the sections  $L_1$  and  $L_4$  are taken into a consideration. The possible difference in wall thicknesses and the existence of the residual compression stresses in  $L_4$  are considered as is the reduced cross-section at the midpoint of the contracted part of the section  $L_4$ .

The same yield stress is taken into account in both sections although in section  $L_4$  the longitudinal welds are present. This is because the HAZ of the longitudinal welds is not located in the arias with the maximal compression stresses.

The diagram is introduced (see Figure 15) from which the following is concluded.

The calculated maximal compression stresses in both considered cross-sections of the mast section  $L_4$  do not reach the yielding stress in the valid diapason of the crane force  $F_z$ . This is true for the point U where the contraction of the section  $L_4$  begins (solid bold curve in Figure 15) and for the location in the middle of the contracted part of the section  $L_4$ , where the cross-section

of the mast profile is reduced (dashed thin curve in Figure 15).

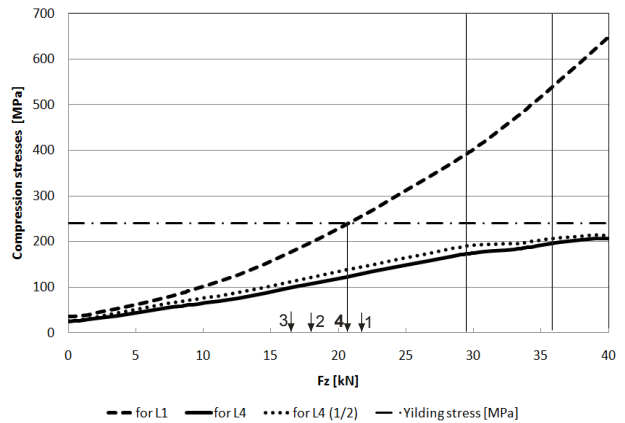


**Figure 15. Compression stresses in walls of the mast sections  $L_1$  and  $L_4$  and the yield stress in these sections**

On the other hand, it is clear that the compression stress in the mast section  $L_1$  (bold dashed curve) increases much quicker (Fig. 15) and reaches the yielding stress at the point marked with the arrow 4 where the extraction force  $F_{z,extr}$  (see (3)) is not yet being developed.

First conclusion from this fact is that the extraction of the spar support is not possible without plasticization of the mast profile in the section  $L_1$  unless if the extraction took place at smaller force  $F_z$  than it is estimated in Section 2.2.

The other conclusion is that in the latter case the appearance of the local buckling without plasticization of the mast profile is possible, because the force  $F_z = 20.6$  kN (see arrow 4 in Figure 15) needed for the plasticization of the cross-section in section  $L_1$  is greater than that needed for local buckling (see arrows 2 and 3 in Figure 15).

## 5. CONCLUSION

The main goal of the paper is to determine whether the assumption that the damage originating from the local buckling of the walls of the mast profile in the highest mast section could be a consequence of the unwanted event when the hook of the auxiliary crane buckled the lateral masts wire-rope.

To determine this possibility, the analytical calculations of the limit loading values for the compression, global buckling, and local buckling were executed. Further, the FEM model was build of the mast – mast wire-ropes system and loaded with the crane force  $F_z$ . The internal loadings obtained with this analysis were further used for calculation of actual stresses in the lowest ( $L_1$ , with the biggest loading) and the highest mast section ( $L_4$ , containing the questionable damage).

During these calculations all the tolerances were used in such a way to calculate the highest strength of the lowest section and the lowest strength of the highest section. With that presumption the calculations are on purpose as much in favour of the main assumption as permissible for scientific researches.

In the calculations the geometry of the mast and the wire-rope system is considered as are the material

properties of the aluminium alloy of the mast and of the stainless steel of the wire-ropes. The changes in material properties of the aluminium alloy in the heat affected zones around the welds are also taken into account. The pre-stress in the wires is considered as well as the residual stresses in the vicinity of the welds. The following is concluded.

Regarding the criterion of the global buckling the main assumption is possible, because no danger of the global buckling is encountered during the loading of the system with the crane force  $F_z$  within the values necessary for the extraction of the spar support which took place during the unwanted crane action ( $29 \text{ kN} \leq F_{z,\text{extr}} \leq 36.5 \text{ kN}$ ).

When the compression criteria is under the observation the results show that the yielding of the aluminium alloy in the highest mast section does not occur as far as the crane force stays inside the calculated limits. On the other hand within this loading limits the yielding can take place in the lowest mast section if the loading exceed the value  $F_z = 20.6 \text{ kN}$ .

The possibility that the main assumption is correct is now smaller but presumed event is possible if the extraction of the spar support can take place at smaller values of  $F_z$  then estimated.

The last criterion is the local buckling criterion. It is proven that the local buckling in both observed mast sections occur before the crane force exceeds  $F_z = 20.6 \text{ kN}$  (when the plasticization of the cross-section of the lowest mast section would happened). This fact leaves the option of the occurrence of the main event open.

On the other hand, the results of calculations show that, despite of favourable usage of input data, the local buckling of the lowest mast section would occur sooner than the local buckling of the highest mast section. This fact alone states that local buckling of the mast profile wall in the highest section cannot take place without local buckling in the lowest section. Because the lowest section of the mast during unwanted event stayed undamaged the further conclusion can be that the main assumption can not be confirmed.

On the other hand, the fact that the crane force values of occurrence of the local buckling are close together ( $F_{z,L1} = 16 \text{ kN}$  and  $F_{z,L4} = 17.5 \text{ kN}$ ) implies the possibility that the main assumption is correct. For this reason further analyses should be done, taking into account the dynamic effects of the impulsive loading and considering more scenarios concerning the position of buckling of the hook, the loading impulse at the moment of extraction of the spar support and option of the sudden release of the hook after that extraction of the spar support.

## REFERENCES

- [1] Boote, D. and Caponetto, M.: Numerical approach to the design of sailing yacht masts, in: *Proceedings of the Tenth Chesapeake Sailing Yacht Symposium – CSYS 1991*, 09.02.1991, Annapolis, USA, p. 59.
- [2] Jatulis, D., Kamaitis, Z. and Juozapaitis, A.: Static behaviour analysis of masts with combined guys,

Journal of Civil Engineering and Management, Vol. 13, No. 3, pp. 177-182, 2007.

- [3] Enlund, H., Pramila, A. and Johansson, P.-G.: Calculated and measured stress resultants in the mast and rigging of a Baltic 39 type yacht, in: *Proceedings of the International Conference on Design Considerations for Small Craft*, 1984, London, UK, pp. 320-332.
- [4] Atkinson, P.: Structural analysis of mast-sail systems using a finite element approach, in: *Conference on Yachting Technology 1987 – Preprints of Papers*, Engineers Australia, Sydney, pp. 59-65, 1987.
- [5] Schoop, H. and Hansel, M.: Structural and aerodynamic calculation of sails as flexible membranes, *Ship Technology Research*, Vol. 44, No. 2, pp. 88-97, 1997.
- [6] DIN 3053 Drahtseile aus Stahldrähten, Spiralseil 1  $\times$  19, 1972.
- [7] *Bamar Catalogue of Aluminium Profiles for Masts*, Bamar UK, Lymington, 1996.
- [8] ISO 6362-2:1990 Wrought Aluminium and Aluminium Alloy Extruded Rods/Bars, Tubes and Profiles, Part 2: Mechanical Properties, 1990.
- [9] Shakeri, M., Mirzaeifar R. and Salehghaffari, S.: New insights into the collapsing of cylindrical thin-walled tubes under axial impact load, *Proceedings of the Institution of Mechanical Engineers, Part C: Journal of Mechanical Engineering Science*, Vol. 221, No. 8, pp. 869-885, 2007.
- [10] Bulson, P.S. (Ed.): *Aluminium Structural Analysis: Recent European Advances*, Taylor & Francis, Abingdon, 1991.

## ЛОКАЛНО ИЗВИЈАЊЕ ТАНКОЗИДОГ АЛУМИНИЈУМСКОГ ЈАРБОЛА

Борис Јерман

У раду је анализиран један од могућих сценарија за појаву локалног извијања зида танкозидог алуминијумског јарбола. Претпостављено је да се кука помоћне дизалице са стрелом, монтиране на пристанишној дизалици са пнеуматичима, закачила за челично уже за бочно ослањање јарбола током њеног премештања са пристаништа. Последице акцидентног дејства дизалице на јарбол једрилице су одређене комбинацијом аналитичких прорачуна и МКЕ. Сложеност јарбола, односно система јарбола и ужади, као и велике деформације и нелинеарне карактеристике материјала су узете у обзир. У оквиру спроведене анализе обухваћена су својства каљене легуре алуминијума као и карактеристике зоне утицаја топлоте у близини варова. На основу израчунатих унутрашњих сила и момената у јарболу и систему ужади разматрана је могућност појаве различитих врста оштећења. Процењена могућа оштећења упоређена су са стварним оштећењима.